Substructure model updating through iterative minimization of modal dynamic residual

Dapeng Zhu, Xinjun Dong, Yang Wang*
School of Civil and Environmental Eng., Georgia Inst. of Technology, Atlanta, GA 30332, USA

ABSTRACT

This research studies a substructure model updating approach. Requiring modal testing data from only part of a large structure (i.e. a substructure), finite element model parameters for the substructure can be updated. Prior to updating, Craig-Bampton transform is adopted to condense the entire structural model into the substructure (currently being instrumented and to be updated) and the residual structure. Finite element model of the substructure remains at high resolution, while dynamic behavior of the residual structure is approximated using only a limited number of dominant mode shapes. To update the condensed structural model, physical parameters in the substructure and modal parameters of the residual structure are chosen as optimization variables; minimization of the modal dynamic residual is chosen as the optimization objective. An iterative linearization procedure is adopted for efficiently solving the optimization problem. The proposed substructure model updating approach is validated through numerical simulation with two plane structures.

Keywords: finite element model updating, substructure updating, modal dynamic residual, iterative least square optimization

1. INTRODUCTION

In order to simulate structural behavior under various operational loading conditions, finite element (FE) models are often constructed. However, in most scenarios, there are usually evident discrepancies between simulation result and the actual structural behavior in the field. The discrepancies are mainly caused by limitations in FE models. For example, many simplifications are adopted in FE modeling, such as idealized hinges and rollers, whereas the simplifications introduce discrepancies from reality. Besides, FE models generally adopt nominal material properties, while the actual properties may have changed over time. Therefore, for higher simulation accuracy, it is essential to update the finite element model based on experimental measurements on the actual structure.

Numerous FE model updating algorithms have been developed and practically applied in the past few decades [1]. Most algorithms can be categorized into two groups, i.e. frequency-domain approaches and time-domain approaches. Frequency-domain approaches update an FE model using frequency-domain structural characteristics extracted from experimental measurement, such as vibration modes [2, 3]. Time-domain approaches directly utilize measured time histories for model updating [4, 5]. Nevertheless, when applied to a high-resolution FE model of a large structure, many existing algorithms suffer computational challenges and convergence problem. The difficulties come from the fact that most of the existing algorithms operate on an entire structural model with very large amount of degrees of freedom (DOFs).

In order to address the computational difficulty, particularly to accommodate data collected at dense measurement locations on large structures, some research activities have been devoted to substructure model updating. As an example for frequency domain approaches, Link adopts Craig-Bampton transform for substructure modeling, and updates the substructure model by minimizing difference between simulated and experimental modal properties [6, 7]. Other researchers adopt frequency spectra for substructure identification, by minimizing difference between simulated and experimental acceleration spectra in certain frequency range [8-10]. In [11], interface force vectors are estimated using multiple sets of measurement; the difference between multiple estimations is minimized with genetic algorithms for substructure model updating. Among time-domain approaches, Koh *et al*. apply the extended Kalman filter for substructure model updating of a shear-frame structure [12]. Displacement, velocity, and acceleration time histories of

*yang.wang@ce.gatech.edu; phone 1 (404) 894-1851; fax 1 (404) 894-2278

the interface DOFs are required, which may not be practical. Later, Koh *et al*. improve the approach by adopting a "quasi-static displacement" concept, so that only acceleration data of the interface DOFs is required [13]. Trink and Koh follow the formulation in [12], and estimate interface displacement and velocity by numerical integration [14]. Another substructure identification is proposed by Tee *et al*., in the context of first and second order model identification in conjunction with observer/Kalman filter and eigensystem realization [15]. Yuen and Katafygiotis present a substructure identification procedure using Bayesian theorem, without requiring interface measurements or excitation measurements [16]. In addition, the sequential nonlinear least square estimation (SNLSE) method has been explored for substructure model updating [17]. The unknown interface coupling parts on the right hand of the equation of motion are treated as unknown forces, and updated in each time step sequentially with state variables and system parameters. Finally, Hou *et al*. has developed a substructure isolation approach based on virtual distortion method; the approach is validated numerically with a plane frame, and experimentally with a continuous beam [18].

This research investigates substructure updating using frequency domain data. Craig-Bampton transform is adopted to partition a large structure into a substructure being analyzed and a residual structure containing the rest of the DOFs. Finite element model of the substructure remains at high resolution, while dynamic behavior of the residual structure is approximated using only a limit number of dominant mode shapes. As a result, the entire structure model is condensed. To update the condensed structural model, physical parameters in the substructure and modal parameters of the residual structure are chosen as optimization variables, and minimization of the modal dynamic residual is chosen as the optimization objective. An iterative linearization procedure is adopted for efficiently solving the optimization problem [3, 19, 20]. The approach is previously validated with a simple spring-mass model. This research attempts to validate the approach with more complicated plane structures.

The rest of the paper is organized as follows. Section 2 presents the formulation of substructure modeling and model updating through modal dynamic residual approach. Section 3 describes numerical investigations on a plane truss and a plane portal frame. The performance of the proposed approach is compared with a conventional updating procedure minimizing experimental and simulated modal property difference. Finally, a summary and discussion are provided.

2. SUBSTRUCTURE MODELING AND UPDATING

This section presents the basic formulation for substructure updating. Section 2.1 describes substructure modeling strategy following Craig-Bampton transform. Section 2.2 describes substructure model updating through minimization of modal dynamic residual.

2.1 Substructure modeling

Figure 1 illustrates the substructure modeling strategy following Craig-Bampton transform [6]. Subscripts *s*, *i*, and *r* are used to denote DOFs associated with the substructure being analyzed, the interface nodes, and the residual structure, respectively. The block-bidiagonal structural stiffness and mass matrices, **K** and **M**, can be assembled using original DOFs $\mathbf{x} = \begin{bmatrix} \mathbf{x}_s & \mathbf{x}_i & \mathbf{x}_r \end{bmatrix}^{\mathrm{T}}$.

$$\mathbf{K} = \begin{bmatrix} \begin{bmatrix} \mathbf{K}_S \end{bmatrix} & \mathbf{0} \\ \mathbf{0} & \mathbf{0} \end{bmatrix} + \begin{bmatrix} \mathbf{0} & \mathbf{0} & \mathbf{0} \\ \mathbf{0} & \begin{bmatrix} \mathbf{K}_R \end{bmatrix} \end{bmatrix} = \begin{bmatrix} \begin{bmatrix} \mathbf{K}_{ss} & \mathbf{K}_{si} \\ \mathbf{K}_{is} & \mathbf{K}_{ii}^S \end{bmatrix} & \mathbf{0} \\ \mathbf{0} & \mathbf{0} \end{bmatrix} + \begin{bmatrix} \mathbf{0} & \mathbf{0} & \mathbf{0} \\ \mathbf{0} & \begin{bmatrix} \mathbf{K}_{ii}^R & \mathbf{K}_{ir} \\ \mathbf{K}_{ri} & \mathbf{K}_{rr} \end{bmatrix} \end{bmatrix} \tag{1}$$

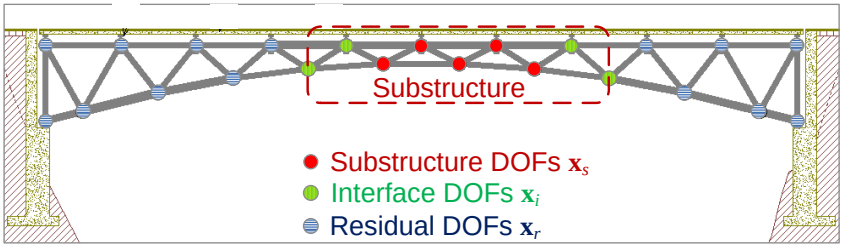

Figure 1. Illustration of substructure modeling strategy.

$$\mathbf{M}=\begin{bmatrix}\begin{bmatrix}\mathbf{M}_S\end{bmatrix} & \mathbf{0}\\ \mathbf{0} & \mathbf{0}\end{bmatrix}+\begin{bmatrix}\mathbf{0} & \mathbf{0}\\ \mathbf{0} & \begin{bmatrix}\mathbf{M}_R\end{bmatrix}\end{bmatrix}=\begin{bmatrix}\begin{bmatrix}\mathbf{M}_{ss} & \mathbf{M}_{si}\\ \mathbf{M}_{is} & \mathbf{M}_{ii}^S\end{bmatrix} & \mathbf{0}\\ \mathbf{0} & \mathbf{0}\end{bmatrix}+\begin{bmatrix}\mathbf{0} & \mathbf{0}\\ \mathbf{0} & \begin{bmatrix}\mathbf{M}_{ii}^R & \mathbf{M}_{ir}\\ \mathbf{M}_{ri} & \mathbf{M}_{rr}\end{bmatrix}\end{bmatrix} \tag{2}$$

Here $\mathbf{K}_S$ and $\mathbf{M}_S$ denote entries of the stiffness and mass matrices corresponding to the substructure; $\mathbf{K}_R$ and $\mathbf{M}_R$ denote entries corresponding to the residual structure; $\mathbf{K}_{ii}^S$ and $\mathbf{M}_{ii}^S$ denote the entries at the interface DOFs and contributed by the substructure; $\mathbf{K}_{ii}^R$ and $\mathbf{M}_{ii}^R$ denote entries at the interface DOFs and contributed by the residual structure.

The dynamic behavior of the residual structure can be approximated using Craig-Bampton formulation [6]. The DOFs of the residual structure, $\mathbf{x}_r \in \mathbb{R}^{n_r}$, are approximated by a linear combination of interface DOFs, $\mathbf{x}_i \in \mathbb{R}^{n_i}$, and modal coordinates of the residual structure, $\mathbf{q}_r \in \mathbb{R}^{n_q}$.

$$\mathbf{x}_r \approx \mathbf{T}\mathbf{x}_i + \mathbf{\Phi}_r \mathbf{q}_r \tag{3}$$

Here $\mathbf{T} = -\mathbf{K}_{rr}^{-1}\mathbf{K}_{ri}$ is the Guyan static condensation matrix; $\mathbf{\Phi}_r = \left[\boldsymbol{\varphi}_1, ..., \boldsymbol{\varphi}_{n_q}\right]$ represents the mode shapes of the residual structure with interface DOFs fixed. The eigenvalue equation providing the mode shapes $\mathbf{\Phi}_r$ and modal frequencies ω_r can be written as

$$\left(-\omega_{r,j}{}^2\mathbf{M}_{rr} + \mathbf{K}_{rr}\right)\boldsymbol{\varphi}_j = 0, \qquad j = 1, ..., n_q \tag{4}$$

Although the size of the residual structure may be large, the number of modal coordinates, n_q, can be chosen as relatively small to reflect the first few dominant mode shapes only (i.e. $n_q << n_r$). The coordinate transformation is rewritten in vector form as:

$$\begin{bmatrix}\mathbf{x}_i\\ \mathbf{x}_r\end{bmatrix} \approx \mathbf{\Gamma}\begin{bmatrix}\mathbf{x}_i\\ \mathbf{q}_r\end{bmatrix}, \text{ where } \quad \mathbf{\Gamma} = \begin{bmatrix}\mathbf{I} & \\ \mathbf{T} & \mathbf{\Phi}_r\end{bmatrix} \tag{5}$$

Suppose $\tilde{\mathbf{K}}_R$ and $\tilde{\mathbf{M}}_R$ denote the new stiffness and mass matrices of the residual structure after transformation:

$$\tilde{\mathbf{K}}_R = \mathbf{\Gamma}^{\mathrm{T}}\mathbf{K}_R\mathbf{\Gamma} \qquad\qquad \tilde{\mathbf{M}}_R = \mathbf{\Gamma}^{\mathrm{T}}\mathbf{M}_R\mathbf{\Gamma} \tag{6}$$

Link described a model updating method for both the substructure and the residual structure [7]. The substructure model is updated as

$$\mathbf{K}_S = \mathbf{K}_{S0} + \sum_{j=1}^{n_\alpha} \alpha_j \mathbf{K}_{S0,j} \qquad\qquad \mathbf{M}_S = \mathbf{M}_{S0} + \sum_{j=1}^{n_\beta} \beta_j \mathbf{M}_{S0,j} \tag{7}$$

where $\mathbf{K}_{S0}$ and $\mathbf{M}_{S0}$ are the stiffness and mass matrices of the substructure and used as initial starting point in the model updating; α_j and β_j correspond to physical system parameters to be updated, such as elastic modulus and density of each substructure element; n_α and n_β represent the total number of corresponding parameters to be updated; $\mathbf{K}_{S0,j}$ and $\mathbf{M}_{S0,j}$ are constant matrices determined by the type and location of these parameters. Subscript "0" will be used hereinafter to denote variables associated with the initial structural model, which serves as the starting point for model updating.

The matrices of the condensed residual structural model, $\tilde{\mathbf{K}}_R$ and $\tilde{\mathbf{M}}_R$ in Eq.(6), each contains $(n_i + n_q) \times (n_i + n_q)$ number of entries. Assuming that physical changes in the residual structure do not significantly alter the generalized eigenvectors of $\tilde{\mathbf{K}}_R$ and $\tilde{\mathbf{M}}_R$, only $(n_i + n_q)$ number of modal parameters are selected as updating parameters for each condensed matrix of the residual structural model :

$$\tilde{\mathbf{K}}_R = \tilde{\mathbf{K}}_{R0} + \sum_{j=1}^{n_i+n_q} \zeta_j \tilde{\mathbf{K}}_{R0,j} \qquad\qquad \tilde{\mathbf{M}}_R = \tilde{\mathbf{M}}_{R0} + \sum_{j=1}^{n_i+n_q} \eta_j \tilde{\mathbf{M}}_{R0,j} \tag{8}$$

where ζ_j and η_j are the modal parameters to be updated; $\tilde{\mathbf{K}}_{R0}$ and $\tilde{\mathbf{M}}_{R0}$ are the initial stiffness and mass matrices of the condensed residual structure model; $\tilde{\mathbf{K}}_{R0,j}$ and $\tilde{\mathbf{M}}_{R0,j}$ represent the constant correction matrices formulated using modal back-transform [7]. Detailed formulation can also be found in [20].

Using all model matrices to be updated, i.e. Eq. (7) for substructure and Eq. (8) for residual structure, the condensed entire structural model with reduced DOFs, $\begin{bmatrix}\mathbf{x}_s & \mathbf{x}_i & \mathbf{q}_r\end{bmatrix}^{\mathrm{T}}$, can be updated with variables α_j, β_j, ζ_j and η_j. For brevity, these variables will be referred to in vector form as $\boldsymbol{\alpha} \in \mathbb{R}^{n_\alpha}$, $\boldsymbol{\beta} \in \mathbb{R}^{n_\beta}$, $\boldsymbol{\zeta} \in \mathbb{R}^{n_i+n_q}$ and $\boldsymbol{\eta} \in \mathbb{R}^{n_i+n_q}$.

$$\tilde{\mathbf{K}} = \tilde{\mathbf{K}}_0 + \sum_{j=1}^{n_\alpha} \alpha_j \begin{bmatrix} \begin{bmatrix} & \mathbf{K}_{S0,j} & \end{bmatrix} & \mathbf{0} \\ \mathbf{0} \quad \mathbf{0} & \mathbf{0} \end{bmatrix} + \sum_{j=1}^{n_i+n_q} \zeta_j \begin{bmatrix} \mathbf{0} & \mathbf{0} & \mathbf{0} \\ \mathbf{0} & \begin{bmatrix} & \tilde{\mathbf{K}}_{R0,j} & \end{bmatrix} \\ \mathbf{0} & \end{bmatrix} = \tilde{\mathbf{K}}_0 + \sum_{j=1}^{n_\alpha} \alpha_j \mathbf{S}_{\alpha,j} + \sum_{j=1}^{n_i+n_q} \zeta_j \mathbf{S}_{\zeta,j} \tag{9}$$

$$\tilde{\mathbf{M}} = \tilde{\mathbf{M}}_0 + \sum_{j=1}^{n_\beta} \beta_j \begin{bmatrix} \begin{bmatrix} & \mathbf{M}_{S0,j} & \end{bmatrix} & \mathbf{0} \\ \mathbf{0} \quad \mathbf{0} & \mathbf{0} \end{bmatrix} + \sum_{j=1}^{n_i+n_q} \eta_j \begin{bmatrix} \mathbf{0} & \mathbf{0} & \mathbf{0} \\ \mathbf{0} & \begin{bmatrix} & \tilde{\mathbf{M}}_{R0,j} & \end{bmatrix} \\ \mathbf{0} & \end{bmatrix} = \tilde{\mathbf{M}}_0 + \sum_{j=1}^{n_\alpha} \beta_j \mathbf{S}_{\beta,j} + \sum_{j=1}^{n_i+n_q} \eta_j \mathbf{S}_{\eta,j} \tag{10}$$

where $\mathbf{S}_{\alpha,j}$, $\mathbf{S}_{\beta,j}$, $\mathbf{S}_{\zeta,j}$ and $\mathbf{S}_{\eta,j}$ represent the sensitivity matrices corresponding to variables α_j, β_j, ζ_j and η_j, respectively.

2.2 Substructure model updating through minimization of modal dynamic residual

To update the substructure model, a modal dynamic residual approach is proposed in this study. It is assumed that sensors are deployed on the substructure and interface DOFs at high density, so that mode shapes in the substructure area can be identified from experimental data. Sensor instrumentation at the residual DOFs is not required. The model updating approach attempts to minimize modal dynamic residual of the generalized eigenvalue equation.

$$\begin{aligned} \underset{\boldsymbol{\alpha},\boldsymbol{\beta},\boldsymbol{\zeta},\boldsymbol{\eta},\boldsymbol{\psi}_{\mathrm{u}}}{\text{minimize}} \quad & \sum_{j=1}^{n_{\mathrm{m}}} \left\| \left(\tilde{\mathbf{K}}(\boldsymbol{\alpha},\boldsymbol{\zeta}) - \omega_j^2 \tilde{\mathbf{M}}(\boldsymbol{\beta},\boldsymbol{\eta}) \right) \begin{Bmatrix} \boldsymbol{\psi}_{\mathrm{m},j} \\ \boldsymbol{\psi}_{\mathrm{u},j} \end{Bmatrix} \right\|^2 \\ \text{subject to} \quad & \boldsymbol{\alpha}_L \le \boldsymbol{\alpha} \le \boldsymbol{\alpha}_U; \quad \boldsymbol{\beta}_L \le \boldsymbol{\beta} \le \boldsymbol{\beta}_U; \quad \boldsymbol{\zeta}_L \le \boldsymbol{\zeta} \le \boldsymbol{\zeta}_U; \quad \boldsymbol{\eta}_L \le \boldsymbol{\eta} \le \boldsymbol{\eta}_U \end{aligned} \tag{11}$$

where $\|\bullet\|$ denotes any vector norm; n_{m} denotes the number of measured modes from experiments; ω_j denotes the j-th modal frequency extracted from experimental data; $\boldsymbol{\psi}_{\mathrm{m},j}$ denotes the entries in the j-th mode shape that correspond to measured (instrumented) DOFs; $\boldsymbol{\psi}_{\mathrm{u},j}$ correspond to unmeasured DOFs; $\boldsymbol{\alpha}$, $\boldsymbol{\beta}$, $\boldsymbol{\zeta}$ and $\boldsymbol{\eta}$ are the system parameters to be updated (see Eq. (9) and (10)). $\boldsymbol{\alpha}_L$, $\boldsymbol{\beta}_L$, $\boldsymbol{\zeta}_L$ and $\boldsymbol{\eta}_L$ denote the lower bounds for vectors $\boldsymbol{\alpha}$, $\boldsymbol{\beta}$, $\boldsymbol{\zeta}$ and $\boldsymbol{\eta}$, respectively; $\boldsymbol{\alpha}_U$, $\boldsymbol{\beta}_U$, $\boldsymbol{\zeta}_U$ and $\boldsymbol{\eta}_U$ denote the upper bounds for vectors $\boldsymbol{\alpha}$, $\boldsymbol{\beta}$, $\boldsymbol{\zeta}$ and $\boldsymbol{\eta}$, respectively. Note that the sign "≤" in Eq. (11) is overloaded to represent element-wise inequality. In summary, ω_j and $\boldsymbol{\psi}_{\mathrm{m},j}$ are extracted from experimental data, and thus, are constant in the optimization problem. The optimization variables are $\boldsymbol{\alpha}$, $\boldsymbol{\beta}$, $\boldsymbol{\zeta}$, $\boldsymbol{\eta}$ and $\boldsymbol{\psi}_{\mathrm{u}}$. Eq. (11) leads to a complex nonlinear optimization problem that is generally difficult to solve. However, if mode shapes at unmeasured DOFs, $\boldsymbol{\psi}_{\mathrm{u}}$, were known, Eq. (11) becomes a convex optimization problem[20, 21]. The optimization variables are system parameters ($\boldsymbol{\alpha}$, $\boldsymbol{\beta}$, $\boldsymbol{\zeta}$ and $\boldsymbol{\eta}$), and the problem can be efficiently solved. Likewise, if system parameters ($\boldsymbol{\alpha}$, $\boldsymbol{\beta}$, $\boldsymbol{\zeta}$ and $\boldsymbol{\eta}$) were known, Eq. (11) also becomes a convex optimization problem with variable $\boldsymbol{\psi}_{\mathrm{u}}$. Therefore, an iterative linearization procedure for efficiently solving the optimization problem is adopted in this study, similar to [3]. Figure 2 shows the pseudo code of the procedure. Each iteration step involves two operations, modal expansion and parameter updating.

(i) Modal expansion

At each iteration, the operation (i) is essentially modal expansion for unmeasured DOFs, where system parameters ($\boldsymbol{\alpha}$, $\boldsymbol{\beta}$, $\boldsymbol{\zeta}$ and $\boldsymbol{\eta}$) are treated as constant. At the first iteration step, these parameter values are based on initial estimation. At later

start with $\boldsymbol{\alpha}$, $\boldsymbol{\beta}$, $\boldsymbol{\zeta}$ and $\boldsymbol{\eta}$ = 0 (meaning $\mathbf{M}$ and $\mathbf{K}$ start with $\mathbf{M}_0$ and $\mathbf{K}_0$) ;
REPEAT {
(i) hold $\boldsymbol{\alpha}$, $\boldsymbol{\beta}$, $\boldsymbol{\zeta}$ and $\boldsymbol{\eta}$ as constant and minimize over variable $\boldsymbol{\psi}_{\mathrm{u}}$;
(ii) hold $\boldsymbol{\psi}_{\mathrm{u}}$ as constant and minimize over variables $\boldsymbol{\alpha}$, $\boldsymbol{\beta}$, $\boldsymbol{\zeta}$ and $\boldsymbol{\eta}$;
} UNTIL convergence ;

Figure 2. Pseudo code of the iterative linearization procedure.

iteration steps, the parameter values are obtained from model updating results in the previous iteration. When model parameters are held constant, $\boldsymbol{\psi}_{\mathrm{u}}$ becomes the only optimization variable in Eq. (11). Arbitrary vector norm functions can be adopted, and the optimization problem can be conveniently coded and efficiently solved using off-the-shelf solvers such as [22]. When Euclidean norm (2-norm) is adopted, the optimization problem without constraints is equivalent to a least square form. The unknown part of the *j*-th experimental mode shape vector, $\boldsymbol{\psi}_{\mathrm{u},j}$, is obtained from following least-square problem.

$$\begin{bmatrix}\mathbf{D}_{j,\mathrm{mu}}\\ \mathbf{D}_{j,\mathrm{uu}}\end{bmatrix}\boldsymbol{\psi}_{\mathrm{u},j} = -\begin{bmatrix}\mathbf{D}_{j,\mathrm{mm}}\\ \mathbf{D}_{j,\mathrm{um}}\end{bmatrix}\boldsymbol{\psi}_{\mathrm{m},j} \tag{12}$$

where definition for $\mathbf{D}_j$ comes from the generalized eigenvalue problem.

$$\begin{bmatrix}\mathbf{D}_{j,\mathrm{mm}} & \mathbf{D}_{j,\mathrm{mu}}\\ \mathbf{D}_{j,\mathrm{um}} & \mathbf{D}_{j,\mathrm{uu}}\end{bmatrix} = \begin{bmatrix}\mathbf{D}_j\end{bmatrix} = \tilde{\mathbf{K}}(\boldsymbol{\alpha},\boldsymbol{\zeta}) - \omega_j^2\tilde{\mathbf{M}}(\boldsymbol{\beta},\boldsymbol{\eta}) \tag{13}$$

Here $\tilde{\mathbf{K}}$ and $\tilde{\mathbf{M}}$ are matrices assembled according to Eq. (9) and (10). In operation (i), the matrices are constant because system parameters ($\boldsymbol{\alpha}$, $\boldsymbol{\beta}$, $\boldsymbol{\zeta}$ and $\boldsymbol{\eta}$) are held constant.

(ii) Parameter updating

The operation (ii) at each iteration is the updating of model parameters ($\boldsymbol{\alpha}$, $\boldsymbol{\beta}$, $\boldsymbol{\zeta}$ and $\boldsymbol{\eta}$) using the expanded complete mode shapes. Thus, $\boldsymbol{\psi}_{\mathrm{u}}$ is held as constant in operation (ii). Again, the optimization problem with $\boldsymbol{\alpha}$, $\boldsymbol{\beta}$, $\boldsymbol{\zeta}$ and $\boldsymbol{\eta}$ as optimization variables can be efficiently solved for arbitrary vector norm function in Eq. (11). When 2-norm is adopted, the problem without constraints is equivalent to a least square form shown below.

$$\begin{bmatrix}
\mathbf{S}_{\alpha,1}\boldsymbol{\psi}_1\cdots\mathbf{S}_{\alpha,n_\alpha}\boldsymbol{\psi}_1 & \mathbf{S}_{\zeta,1}\boldsymbol{\psi}_1\cdots\mathbf{S}_{\zeta,n_\mathrm{l}+n_\mathrm{q}}\boldsymbol{\psi}_1 & -\omega_1^2\mathbf{S}_{\beta,1}\boldsymbol{\psi}_1\cdots-\omega_1^2\mathbf{S}_{\beta,n_\beta}\boldsymbol{\psi}_1 & -\omega_1^2\mathbf{S}_{\eta,1}\boldsymbol{\psi}_1\cdots-\omega_1^2\mathbf{S}_{\eta,n_\mathrm{l}+n_\mathrm{q}}\boldsymbol{\psi}_1\\
\mathbf{S}_{\alpha,1}\boldsymbol{\psi}_2\cdots\mathbf{S}_{\alpha,n_\alpha}\boldsymbol{\psi}_2 & \mathbf{S}_{\zeta,1}\boldsymbol{\psi}_2\cdots\mathbf{S}_{\zeta,n_\mathrm{l}+n_\mathrm{q}}\boldsymbol{\psi}_2 & -\omega_2^2\mathbf{S}_{\beta,1}\boldsymbol{\psi}_2\cdots-\omega_2^2\mathbf{S}_{\beta,n_\beta}\boldsymbol{\psi}_2 & -\omega_2^2\mathbf{S}_{\eta,1}\boldsymbol{\psi}_2\cdots-\omega_2^2\mathbf{S}_{\eta,n_\mathrm{l}+n_\mathrm{q}}\boldsymbol{\psi}_2\\
\vdots & \vdots & \vdots & \vdots\\
\mathbf{S}_{\alpha,1}\boldsymbol{\psi}_{n_m}\cdots\mathbf{S}_{\alpha,n_\alpha}\boldsymbol{\psi}_{n_m} & \mathbf{S}_{\zeta,1}\boldsymbol{\psi}_{n_m}\cdots\mathbf{S}_{\zeta,n_\mathrm{l}+n_\mathrm{q}}\boldsymbol{\psi}_{n_m} & -\omega_{n_m}^2\mathbf{S}_{\beta,1}\boldsymbol{\psi}_{n_m}\cdots-\omega_{n_m}^2\mathbf{S}_{\beta,n_\beta}\boldsymbol{\psi}_{n_m} & -\omega_{n_m}^2\mathbf{S}_{\eta,1}\boldsymbol{\psi}_{n_m}\cdots-\omega_{n_m}^2\mathbf{S}_{\eta,n_\mathrm{l}+n_\mathrm{q}}\boldsymbol{\psi}_{n_m}
\end{bmatrix}\begin{Bmatrix}\boldsymbol{\alpha}\\ \boldsymbol{\beta}\\ \boldsymbol{\zeta}\\ \boldsymbol{\eta}\end{Bmatrix} = \begin{Bmatrix}\left(\omega_1^2\tilde{\mathbf{M}}_0-\tilde{\mathbf{K}}_0\right)\boldsymbol{\psi}_1\\ \left(\omega_2^2\tilde{\mathbf{M}}_0-\tilde{\mathbf{K}}_0\right)\boldsymbol{\psi}_2\\ \vdots\\ \left(\omega_{n_m}^2\tilde{\mathbf{M}}_0-\tilde{\mathbf{K}}_0\right)\boldsymbol{\psi}_{n_m}\end{Bmatrix} \tag{14}$$

Here $\mathbf{S}_{\alpha,j}$, $\mathbf{S}_{\beta,j}$, $\mathbf{S}_{\zeta,j}$ and $\mathbf{S}_{\eta,j}$ represent the constant sensitivity matrices from Eq. (9) and (10). $\boldsymbol{\psi}_j$ is the *j*-th expanded mode containing both measured and unmeasured DOFs.

$$\boldsymbol{\psi}_j = \begin{Bmatrix}\boldsymbol{\psi}_{\mathrm{m},j}\\ \boldsymbol{\psi}_{\mathrm{u},j}\end{Bmatrix} \tag{15}$$

3. NUMERICAL EXAMPLES

To validate the proposed approach for substructure model updating, two numerical examples are studied. Section 3.1 describes a plane truss example, and Section 3.2 describes a plane portal frame example. For comparison, substructure model updating is also performed using a conventional approach that minimizes experimental and simulated modal

property difference [7]. The conventional model updating formulation aims to minimize the difference between experimental and simulated natural frequencies, as well as the difference between experimental and simulated mode shapes of the substructure.

$$\underset{\boldsymbol{\alpha},\boldsymbol{\beta},\boldsymbol{\zeta},\boldsymbol{\eta}}{\text{minimize}} \quad \sum_{j=1}^{n_m}\left\{\left(\frac{\omega_j^{\text{FE}}-\omega_j}{\omega_j}\right)^2+\left(\frac{1-\sqrt{\text{MAC}_j}}{\sqrt{\text{MAC}_j}}\right)^2\right\} \tag{16}$$

where ω_j^{FE} and ω_j represent the j-th simulated (from the condensed model in Eq. (9) and (10)) and experimentally extracted frequencies, respectively; MAC_j represents the modal assurance criterion evaluating the difference between the j-th simulated and experimental mode shapes. Note that mode shape entries only corresponding to measured DOFs are compared (i.e. between $\boldsymbol{\psi}_{\text{m},j}^{\text{FE}}$ and $\boldsymbol{\psi}_{\text{m},j}$). A nonlinear least-square optimization solver, '`lsqnonlin`' in MATLAB toolbox [23], is adopted to numerically solve the optimization problem minimizing modal property difference. The optimization solver seeks a minimum through Levenberg-Marquardt algorithm, which adopts a search direction interpolated between the Gauss-Newton direction and the steepest descent direction [24].

3.1 Plane truss structure

Figure 3 shows the plane truss model for validating the proposed substructure updating approach. The truss model has 26 nodes, and each node has two translational DOFs. Horizontal and vertical springs (k_{x1} and k_{y1}) are allocated at the left support to simulate a non-ideal hinge, while a vertical spring (k_{y2}) is allocated at the right support to simulate a non-ideal roller. Table 1 summarizes the structural properties of the model, including elastic modulus E_1 of top-level truss bars, modulus E_2 of diagonal and vertical bars, modulus E_3 of bottom bars, and three spring stiffness numbers. The table provides initial nominal values for all parameters, as starting point for model updating. The table also lists actual values, which ideally are to be identified. The relative changes from initial to actual values are also listed.

A substructure containing first three truss units from left is selected for model updating (Figure 3). The selected substructure contains six substructure nodes and two interface nodes. Each node includes two translational DOFs, so the substructure DOFs $\mathbf{x}_s \in \mathbb{R}^{12\times1}$ and the interface DOFs $\mathbf{x}_i \in \mathbb{R}^{4\times1}$. It is assumed all substructure and interface DOFs are instrumented with sensors for experimentally capturing substructure vibration modes. No measurement is required on the residual structure. For modeling, dynamic response of the residual structure is approximated using ten modal coordinates, i.e. $n_q = 10$ in Eq.(3). As a result, the entire structural model is condensed to $n_s+n_i+n_q=26$ DOFs (from 52 DOFs in the original structure). Without loss of generality, accurate structural mass matrix is assumed to be known, so mass parameters $\boldsymbol{\beta}$ (Eq. (7)) is not among the updating parameters. The substructure stiffness parameters $\boldsymbol{\alpha}$ (being updated) include the three elastic moduli in the substructure (E_1, E_2, and E_3), as well as the spring stiffness values at the left support (k_{x1} and k_{y1}). Because the spring stiffness at the right support, k_{y2}, only contributes to residual structure, k_{y2}

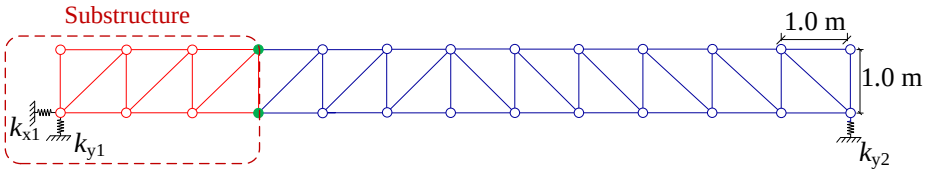

Figure 3. Substructure modeling of a plane truss

Table 1. Structural properties

Update parameter	Steel elastic modulus (10^{11} N/m^2)			k_{x1} (10^6 N/m)	k_{y1} (10^6 N/m)	k_{y2} (10^6 N/m)
	Top (E_1)	Diag. & Vert. (E_2)	Bottom (E_3)			
Initial value	2	2	2	5	5	5
Actual value	2.2	2.1	1.9	2	7	7
Change (%)	10%	5%	-5%	-60%	40%	40%

cannot be updated. Instead, the residual structure is updated through modal parameters of the residual structure with free interface (ζ_2, ζ_3, ..., ζ_{14} and η_1, η_2, ..., η_{14}). Note that $n_i+n_q = 14$ and that the modal parameter ζ_1 is not included, because the first resonance frequency of the residual structure with free interface is zero (corresponding to free-body movement). As a result, the first modal correction matrix $\tilde{\mathbf{K}}_{R0,1}$ in Eq.(8) is a zero matrix, and so is the corresponding sensitivity matrix $\mathbf{S}_{\zeta,1}$. Using modal frequencies and substructure mode shapes (ω_j and $\boldsymbol{\psi}_{\mathrm{m},j}$) as "experimental data", both the proposed modal dynamic residual approach and the conventional modal property difference approach are applied for substructure model updating. For each approach, the updating is performed assuming different numbers of measured modes are available (i.e. modes corresponding to the 3~6 lowest natural frequencies).

Table 2. Updated parameter changes (%) for substructure elements by minimization of modal dynamic residual

Stiffness change	Steel elastic modulus change (%)			Change in k_{x1} (%)	Change in k_{y1} (%)
	Top (E_1)	Diag. & Vert. (E_2)	Bottom (E_3)		
3 modes	10.08	5.03	-5.02	-60.00	40.04
4 modes	9.99	5.00	-5.00	-60.00	40.00
5 modes	9.99	4.99	-4.98	-60.00	39.99
6 modes	10.04	4.99	-4.98	-60.00	39.99

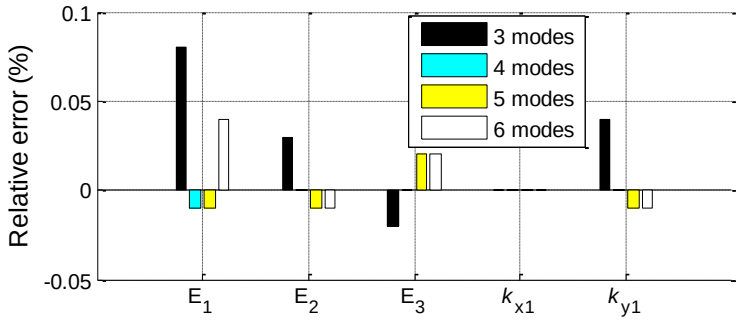

Figure 4. Relative errors of the updated parameters by minimization of modal dynamic residual

Table 3. Updated parameter changes (%) for substructure elements by minimization of modal property difference

Stiffness change	Steel elastic modulus change (%)			Change in k_{x1} (%)	Change in k_{y1} (%)
	Top (E_1)	Diag. & Vert. (E_2)	Bottom (E_3)		
3 modes	5.23	2.84	-7.86	-60.2	37.02
4 modes	7.71	4.59	-4.58	-58.44	38.90
5 modes	2.03	7.70	-5.88	-57.82	38.23
6 modes	4.33	7.74	0.16	-55.43	41.11

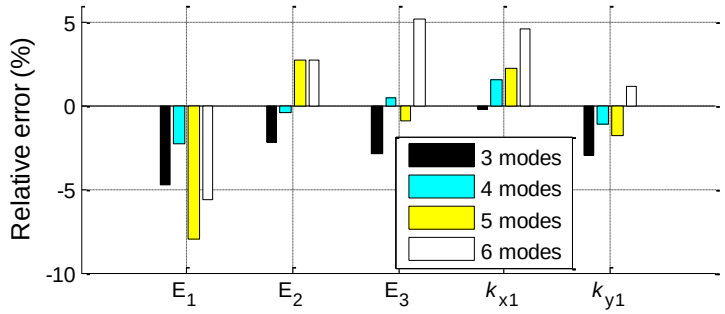

Figure 5. Relative errors of the updated parameters by minimization of modal property difference

Table 2 summarizes the updating results using the proposed modal dynamic residual approach for substructure model updating. The results are presented in terms of relative change percentages from initial values. For every available number of modes, the updating parameter changes are close to the ideal percentages listed in Table 1. Figure 4 plots the relative errors of the updating results, i.e. deviation from the actual values, for different number of available modes. The figure shows that the updating results accurately identify all substructure properties, and the maximum updating error is a negligible 0.08% for parameter E_1 (when only three modes are available).

Similarly, Table 3 summarizes the updating results using the conventional modal property difference approach. The updated parameter changes are apparently different from the ideal percentages list in Table 1. Figure 5 shows the relative errors of the updating results, as compared to the actual values. The conventional approach can update some structural properties to a fairly good accuracy, but the results are generally worse than the proposed modal dynamic residual approach. The maximum error for conventional modal property difference approach is -7.98% for parameter E_1 (with five available modes). Figure 4 and Figure 5 also show that using either the proposed or the conventional approach, the updating accuracy does not monotonically decrease when number of available modes increases. This is probably caused by the approximations made in the formulation for substructure model updating. First, the Craig-Bampton transform used for model condensation (Eq.(3)) adopts static condensation matrix as the transformation matrix for interface DOFs to residual DOFs, which neglects interface dynamic contribution. Second, the Craig-Bampton transform uses only a few dominant modes describing dynamic behavior of the residual structure. Third, while updating modal parameters for the residual structure, it is assumed that physical parameter changes in the residual structure do not significantly alter the generalized eigenvectors of the residual structural matrices (Eq. (8)). These assumptions may introduce more inaccuracy to the updating process when higher modes are involved.

3.2 Plane portal frame structure

Figure 6 shows the plane portal frame model. The frame model has 42 elements and 131 DOFs in total. The portal frame has a hinge support on each side. Distinct elastic moduli are assigned along frame members as actual values (Figure 6). For example, lower-left corner of the substructure has four elements with the same modulus 0.8E. The upper eight elements at left column at left column have the same modulus 1.0E. In the initial model as starting point of model updating, it is assumed that the same elastic modulus (E) is assigned to all elements.

A substructure at the upper right corner, containing 14 elements, is selected for model updating. The selected substructure contains 13 substructure nodes and 2 interface nodes. Each node has two translational DOFs and one rotational DOF, so the substructure DOFs $\mathbf{x}_s \in \mathbb{R}^{39\times 1}$ and the interface DOFs $\mathbf{x}_i \in \mathbb{R}^{6\times 1}$. It is assumed only translational DOFs at substructure and interface nodes are instrumented with accelerometers for experimentally capturing substructure vibration modes; rotational DOFs are not measured. Again, no measurement is required on the residual structure. Dynamic response of the residual structure is approximated using ten modal coordinates, i.e. $n_q = 10$ in Eq.(3). As a result, the entire structural model is condensed to $n_s+n_i+n_q=55$ DOFs (from 131 DOFs in the original

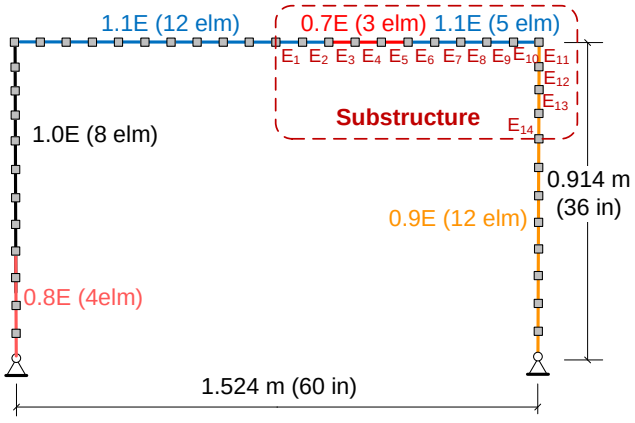

Figure 6. Substructure modeling of a plane portal frame

structure). Similar to the plane truss example, mass parameters **β** is not among the updating variables. The selected updating parameters are the physical parameters **α** (the 14 different elastic moduli of the 14 substructure elements), and modal parameters of the residual structural with free interface (ζ_3, ζ_4, ..., ζ_{16} and η_1, η_2, ..., η_{16}). Note that $n_i+n_q = 16$ and that the modal parameters ζ_1 and ζ_2 are not included, because the first two resonance frequencies of the residual structure with free interface are zero similar as in Section 3.1. Again, for each substructure model updating approach, the updating is performed assuming different numbers of measured modes are available (i.e. modes corresponding to the 3~6 lowest natural frequencies).

Table 4 summarizes the updating results using the presented modal dynamic residual approach for substructure model updating. The results are presented in terms of relative change percentage from initial values. Similar to the truss

Table 4. Updated parameter changes (%) for substructure elements by minimization of modal dynamic residual

Stiffness changes (%)	E_1	E_2	E_3	E_4	E_5	E_6	E_7	E_8	E_9	E_{10}	E_{11}	E_{12}	E_{13}	E_{14}
3 modes	10.59	10.29	-29.92	-29.93	-29.95	10.08	10.05	10.06	10.04	10.06	-9.97	-9.95	-9.95	-9.95
4 modes	14.12	13.21	-28.63	-28.62	-28.82	11.86	11.69	11.73	11.64	11.69	-8.66	-8.58	-8.58	-8.53
5 modes	10.67	10.60	-29.94	-29.89	-29.97	10.10	10.01	10.07	10.02	10.05	-9.98	-9.96	-9.98	-10.02
6 modes	13.16	12.46	-29.08	-29.07	-29.30	10.98	10.84	10.78	10.70	10.67	-9.47	-9.48	-9.47	-9.41

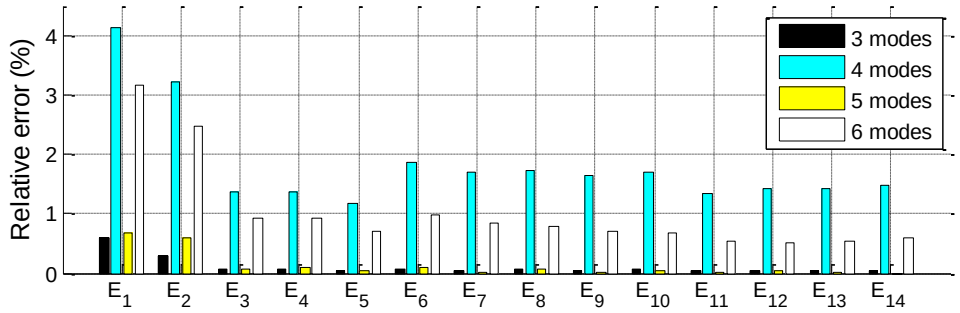

Figure 7. Relative errors of the updated elastic moduli by minimization of modal dynamic residual

Table 5. Updated parameter changes (%) for substructure elements by minimization of modal property difference

Stiffness changes (%)	E_1	E_2	E_3	E_4	E_5	E_6	E_7	E_8	E_9	E_{10}	E_{11}	E_{12}	E_{13}	E_{14}
3 modes	-0.96	-2.18	-3.41	-5.62	-4.26	-2.52	0.02	1.81	2.07	1.14	-0.39	-1.75	-2.04	-1.29
4 modes	0.42	0.05	-0.26	-1.25	-0.82	-1.50	-1.26	-0.48	-0.17	0.43	0.48	0.44	-0.43	-0.61
5 modes	1.15	-0.88	-4.18	-10.79	-10.02	-7.00	-2.31	2.46	0.94	-4.88	-9.78	-6.62	-2.99	0.11
6 modes	4.85	0.28	-1.91	-3.83	-4.49	-2.09	-0.68	-0.56	0.45	-0.02	-1.80	-1.41	-0.27	-1.14

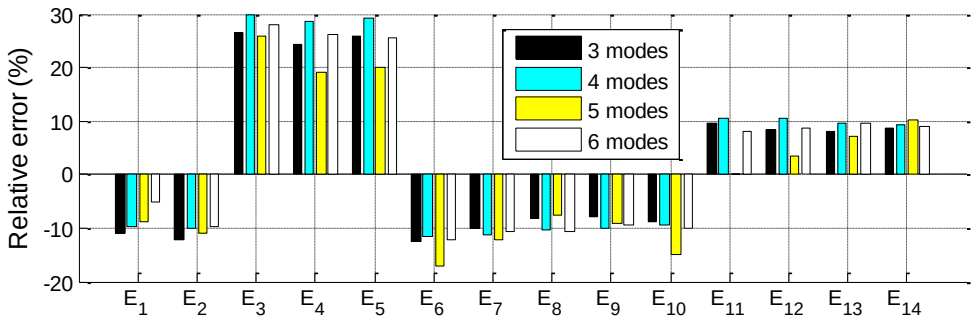

Figure 8. Relative errors of the updated elastic moduli by minimization of modal property difference

example, for every available number of modes, the updating parameter changes are fairly close to the ideal percentages that can be easily calculated from Figure 6, element by element in the substructure. For example, the correct/ideal change should be 10% for E_1, 10% for E_2, -30% for E_3, ect. Figure 7 plots the relative errors of the updating results as compared to the actual values, for different number of available modes. The proposed approach can correctly identify most structural parameters. The larger errors are all with E_1 and E_2, which are close to an interface node. The maximum error is 4.12% (when 4 modes are available), which is higher than the error for the truss structure. Nevertheless, in most scenarios, the majority of the parameters can be identified at less than 2% error. Note that in this example, only translational DOFs of the substructure and interface nodes are measured; rotational DOFs are unmeasured as commonly encountered in practice. While in plane truss example in Section 3.1, all DOFs on substructure and interface nodes are measured. This can be the reason that the results in frame example are less accurate than the results in truss example.

Table 5 summarizes the updating results using the conventional modal property difference approach. The updated parameter changes are apparently different from the correct/ideal values. Figure 8 plots the relative errors of the updating results as compared to the actual values. The figure shows that the updating results from conventional approach have much larger errors than the results from the proposed modal dynamic residual approach (Figure 7). It can be concluded that the conventional approach minimizing modal property difference when used for substructure model updating cannot achieve a reasonable accuracy in this example.

4. SUMMARY & CONCLUSION

This paper studies substructure model updating through minimization of modal dynamic residual. Craig-Bampton transform is adopted to condense the entire structural model into the substructure (currently being instrumented and to be updated) and the residual structure. Finite element model of the substructure remains at high resolution, while dynamic behavior of the residual structure is approximated using only a limited number of dominant mode shapes. To update the condensed structural model, physical parameters in the substructure and modal parameters of the residual structure are chosen as optimization variables; minimization of the modal dynamic residual is chosen as the optimization objective. An iterative linearization procedure is adopted for efficiently solving the optimization problem. The presented substructure updating method is validated through a plane truss example and a plane portal frame example. The proposed approach accurately identifies all structural parameters for the truss example, and most of the parameters for the frame example. For comparison, a conventional modal property difference approach is also applied, and shows much lower accuracy than the proposed modal dynamic residual approach. Future research will continue to investigate the substructure model updating approach on more complicated structural models, through both simulations and experiments.

5. ACKNOWLEDGEMENTS

This research is partially sponsored by the National Science Foundation (#CMMI-1150700 and #CMMI-1041607), the Research and Innovative Technology Administration of US DOT (#DTRT12GUTC12) and Georgia DOT (#RP12-21). Any opinions, findings, and conclusions or recommendations expressed in this publication are those of the authors and do not necessarily reflect the view of the sponsors.

REFERENCES

[1] Friswell, M. I. and Mottershead, J. E., [Finite element model updating in structural dynamics], Kluwer Academic Publishers, Dordrecht, Boston (1995).

[2] Jaishi, B. and Ren, W. X., "Damage detection by finite element model updating using modal flexibility residual," Journal of Sound and Vibration, 290(1-2), 369-387 (2006).

[3] Farhat, C. and Hemez, F. M., “Updating finite element dynamic models using an element-by-element sensitivity methodology,” AIAA Journal, 31(9), 1702-1711 (1993).
[4] Hoshiya, M. and Saito, E., “Structural identification by extended kalman filter,” Journal of Engineering Mechanics-ASCE, 110(12), 1757-1770 (1984).
[5] Yang, J. N., Huang, H. and Pan, S., “Adaptive quadratic sum-squares error for structural damage identification,” Journal of Engineering Mechanics, 135(2), 67-77 (2009).
[6] Craig, R. R., Jr. and Bampton, M. C. C., “Coupling of substructures of dynamics analyses,” AIAA Journal, 6(7), 1313-1319 (1968).
[7] Link, M., “Updating analytical models by using local and global parameters and relaxed optimisation requirements,” Mechanical Systems and Signal Processing, 12(1), 7-22 (1998).
[8] Zhao, Q., Sawada, T., Hirao, K. and Nariyuki, Y., “Localized identification of MDOF structures in the frequency domain,” Earthquake Engineering & Structural Dynamics, 24(3), 325-338 (1995).
[9] Zhang, D. and Johnson, E. A., “Substructure identification for shear structures I: Substructure identification method,” Structural Control and Health Monitoring, 20(5), 804-820 (2013).
[10] Zhang, D. and Johnson, E. A., “Substructure identification for shear structures II: Controlled substructure identification,” Structural Control and Health Monitoring, 20(5), 821-834 (2013).
[11] Koh, C. G. and Shankar, K., “Substructural identification method without interface measurement,” Journal of Engineering Mechanics, 129(7), 769 (2003).
[12] Koh, C. G., See, L. M. and Balendra, T., “Estimation of structural parameters in time domain - a substructure approach,” Earthquake Engineering & Structural Dynamics, 20(8), 787-801 (1991).
[13] Koh, C. G., Hong, B. and Liaw, C. Y., “Substructural and progressive structural identification methods,” Engineering structures, 25(12), 1551-1563 (2003).
[14] Trinh, T. N. and Koh, C. G., “An improved substructural identification strategy for large structural systems,” Structural Control and Health Monitoring, n/a-n/a (2011).
[15] Tee, K. F., Koh, C. G. and Quek, S. T., “Substructural first- and second-order model identification for structural damage assessment,” Earthquake Engineering & Structural Dynamics, 34(15), 1755-1775 (2005).
[16] Yuen, K.-V. and Katafygiotis, L. S., “Substructure identification and health monitoring using noisy response measurements only,” Computer-Aided Civil and Infrastructure Engineering, 21(4), 280-291 (2006).
[17] Yang, J. N. and Huang, H., “Substructure damage identification using damage tracking technique,” Proceedings of SPIE, Sensors and Smart Structures Technologies for Civil, Mechanical, and Aerospace Systems 2007, 6529, 65292R (2007).
[18] Hou, J., Jankowski, Ł. and Ou, J., “A substructure isolation method for local structural health monitoring,” Structural Control and Health Monitoring, 18(6), 601-618 (2011).
[19] Zhu, D., Dong, X. and Wang, Y., "Substructure model updating through modal dynamic residual approach," Proceedings of the 9th International Workshop on Structural Health Monitoring, Stanford, CA, 2013.
[20] Zhu, D. and Wang, Y., "Substructure model updating through iterative convex optimization," Proceeding of the ASME 2012 Conference on Smart Materials, Adaptive Structures and Intelligent Systems (SMASIS 2012), Stone Mountain, GA, USA, 2012.
[21] Boyd, S. P. and Vandenberghe, L., [Convex Optimization], Cambridge University Press, Cambridge, UK ; New York (2004).
[22] Grant, M. and Boyd, S. “CVX: MATLAB software for disciplined convex programming, version 2.0,” (2014, Feb). http://stanford.edu/~boyd/cvx.
[23] MathWorks Inc., [Control System Toolbox : for Uses with MATLAB® : Getting Started], MathWorks Inc., Natick, MA (2005).
[24] Moré, J., "The Levenberg-Marquardt algorithm: Implementation and theory", [Numerical Analysis] (Ed. G. A. Watson), Springer, Berlin, Heidelberg, Germany (1978).